Enhanced porosity preservation by pore fluid overpressure and chlorite grain coatings in the Triassic Skagerrak, Central Graben, North Sea, UK

STEPHAN STRICKER* & STUART J. JONES

Department of Earth Sciences, Durham University, South Road, Durham, DH1 3LE, UK

**Correspondence: stephan.stricker@durham.ac.uk*

Abstract: Current understanding of porosity preservation in deeply buried sandstone reservoirs tends to be focused on how diagenetic grain coatings of clay minerals and microquartz can inhibit macroquartz cementation. However, the importance of overpressure developed during initial (shallow) burial in maintaining high primary porosity during subsequent burial has generally not been appreciated. Where pore fluid pressures are high, and the vertical effective stress is low, the shallow arrest of compaction can allow preservation of high porosity and permeability at depths normally considered uneconomic. The deeply buried fluvial sandstone reservoirs of the Triassic Skagerrak Formation in the Central Graben, North Sea, show anomalously high porosities at depths greater than 3500 metres below sea floor (mbsf). Pore pressures can exceed 80 MPa in the upper part of the Skagerrak Formation at depths of 4000–5000 mbsf, where temperatures are above 140°C. The Skagerrak reservoirs commonly have high primary porosities of up to 35%, little macroquartz cement and variable amounts of diagenetic chlorite grain coats. This research sheds light on the complex controls on reservoir quality in the fluvial sandstones of the Skagerrak Formation by identifying the role of shallow overpressure in arresting mechanical compaction and the importance of chlorite detrital grain coatings in inhibiting macroquartz cement overgrowth as temperature increases during progressive burial.

Deeply buried sandstone reservoirs are the cumulative product of depositional processes and diagenesis during burial both at shallow depths, and at greater depths where temperatures are higher. Simple porosity–depth trends can offer some useful guidance but are not always successful in predicting reservoir porosity. Reservoirs with anomalously high porosities are common in several hydrocarbon basins, e.g. Central Graben, North Sea, UK (Osborne & Swarbrick 1999; Nguyen *et al.* 2013; Grant *et al.* 2014); the Gulf of Mexico, USA (Taylor *et al.* 2004; Ehrenberg *et al.* 2008; Ajdukiewicz *et al.* 2010); the Santos Basin, Brazil (Anjos *et al.* 2003) and the Indus Basin, Pakistan (Berger *et al.* 2009). Current understanding of porosity preservation in deeply buried sandstone reservoirs (>4000 mbsf, metres below sea floor) tends to be focused on how coatings of clay and microquartz on detrital grains can inhibit macroquartz cementation. There are many studies where deep reservoir porosity is linked to early diagenetic clay or microquartz grain coats (Pittman *et al.* 1992; Ehrenberg 1993; Aase *et al.* 1996; Bloch *et al.* 2002; Berger *et al.* 2009; Ajdukiewicz & Lander 2010; Ajdukiewicz & Larese 2012; French *et al.* 2012; Worden *et al.* 2012; Bahlis & De Ros 2013). These studies have proven that quartz-rich sandstones with robust and continuous diagenetic clay or microquartz grain coats contain a much lower volume of macroquartz cement than expected (Berger *et al.* 2009; Ajdukiewicz & Lander 2010).

The role played by fluid overpressure in porosity preservation during the burial of sandstones has often been overlooked or considered less significant (e.g. Audet & McConnell 1992; Gaarenstroom *et al.* 1993; Giles 1997; Bloch *et al.* 2002; Taylor *et al.* 2010). The preservation of enhanced secondary porosity has also been attributed to high overpressures and increased porosity at depth (e.g. Wilkinson *et al.* 1997; Haszeldine *et al.* 1999). Increasing vertical effective stress (VES) caused by sediment loading is the major driver of mechanical compaction and porosity reduction during shallow burial. Pore fluid overpressure reduces the stress on intergranular and cement–grain contacts and inhibits both mechanical compaction and pressure dissolution (Swarbrick & Osborne 1998). The shallow onset of pore fluid overpressure enhances porosity preservation, as noted for the Triassic Skagerrak Formation of the Central North Sea (Nguyen *et al.* 2013; Grant *et al.* 2014).

The Triassic Skagerrak Formation is one of the main reservoirs in the high-pressure high-temperature (HPHT) province in the Central

From: Armitage, P. J., Butcher, A. R., Churchill, J. M., Csoma, A. E., Hollis, C., Lander, R. H., Omma, J. E. & Worden, R. H. (eds) 2018. *Reservoir Quality of Clastic and Carbonate Rocks: Analysis, Modelling and Prediction*. Geological Society, London, Special Publications, **435**, 321–341.
First published online January 5, 2016, https://doi.org/10.1144/SP435.4

Graben, North Sea. Pore pressures can exceed 80 MPa in the upper part of the Skagerrak Formation at depths of 4000–5000 mbsf where temperatures are in the range 166–200°C (Swarbrick *et al.* 2000; di Primio & Neumann 2008; Nguyen *et al.* 2013). Overpressures are widespread in the Mesozoic reservoirs in the Central North Sea, a region that since the early Cretaceous has experienced almost continuous sedimentation of dominantly fine-grained lithologies (Osborne & Swarbrick 1999; Swarbrick *et al.* 2000; Yardley & Swarbrick 2000).

Typical porosity–depth trends for siliciclastic reservoirs, show porosities of 10–15% at depths of 4000–5000 mbsf (Ehrenberg *et al.* 2009). However, the Skagerrak reservoir sandstones retain remarkably good porosity, up to 35%, and a low degree of compaction with respect to their present-day depths of burial. It is these higher-than-expected porosities that form the focus of this study. Here we present new results for the diagenesis and pore pressure evolution of the Triassic Skagerrak Formation in the Josephine High (J-Block), located within the Central Graben in UK Quad 30, and in the Heron field located farther north in UK Quad 22.

Basin analysis and burial history modelling have been undertaken to investigate the role of pore fluid overpressure evolution in the maintenance of high primary porosity during shallow burial (<2500 m burial), where mechanical compaction dominates. The basin model was then compared to petrographic data to investigate the role of palaeopressures in the maintenance of high primary porosity at depth. Detailed SEM and petrographic analysis was then applied to investigate the role of clay mineral grain coatings in maintaining high primary porosity in the high-temperature and diagenetic-controlled deep burial phase (>2500 m burial). This simple approach yields results that allow important inferences to be made about the controls on porosity preservation in HPHT reservoirs. These results complement previous studies in the Central Graben, North Sea (e.g. Nguyen *et al.* 2013; Grant *et al.* 2014) and provide important insights into the controls on reservoir quality of deeply buried sandstones.

Geological setting

The Central Graben of the North Sea is part of the NW–SE-trending southern extension of a trilete rift system (i.e. an incipient ridge–ridge triple junction), with the Viking Graben as the northern arm and the Inner and Outer Moray Firth as the western arm. The North Sea Central Graben is 70–130 km wide with an approximate length of 550 km. The rift system separates the Norwegian basement in the east from the UK continental shelf in the west. The North Sea Central Graben consists of the West and the East Central Graben, divided by the Forties–Montrose and Josephine Ridge horst blocks and flanked by marginal platform areas (Fig. 1). The rift system developed in at least two major rifting phases, one during the Permian–Triassic (290–210 Ma) and the second during the Late Jurassic (155–140 Ma) (Gowers & Sæbøe 1985; Glennie 1998). The geological history has commonly been divided into pre-rift, syn-rift and post-rift phases (Clark *et al.* 1999). Syn-rift sediments are mainly siliciclastic Triassic and Jurassic sediments of up to 2000 m in thickness. The post-rift sediments from the Cretaceous to Holocene are up to 4500 m thick (Fig. 2). Post-rift sediments are mainly siliciclastic rocks dominated by shale, sandstone, silty sandstone and a thick Upper Cretaceous Chalk section (Goldsmith *et al.* 2003). Importantly, Upper Cretaceous Chalk units including the Ekofisk, Tor and Hod Formations (Fig. 2) are the main reservoir seals for the sub-Chalk reservoirs in the Central Graben, North Sea (Mallon & Swarbrick 2002, 2008; Swarbrick *et al.* 2010). These highly cemented and mechanically compacted Chalk units have the potential to seal high overpressure in the underlying highly pressured reservoirs (Mallon *et al.* 2005; Mallon & Swarbrick 2008; Swarbrick *et al.* 2010). After the North Atlantic Ocean opened, the Eocene and younger Hordaland and Nordland groups, comprising up to 2500 m of predominantly siltstone and shale, were deposited.

This study focuses on two key HPHT areas in the Central Graben, North Sea: the Heron Cluster in UK quadrant 22, part of the Eastern Trap Area Project (ETAP) area at the southern end of the Forties–Montrose High; and the J-Block area in UK quadrant 30, located on the Josephine Ridge. Both areas are part of a wider HPHT province that includes the Triassic strata of the Central Graben and the southern part of the Viking Graben (Goldsmith *et al.* 2003; Fig. 1).

Triassic Skagerrak stratigraphy

The Triassic Skagerrak Formation in the Central Graben, North Sea comprises 500–1000 m of predominantly continental braided and meandering fluvial systems and terminal fluvial fans with lacustrine facies (McKie & Audretsch 2005; De Jong *et al.* 2006). The Skagerrak sediments accumulated in a series of fault- and salt-controlled mini-basins, or pods, within the overall rift basin (Smith *et al.* 1993; Matthews *et al.* 2007). The thick Zechstein salt, of late Permian age, strongly influenced sedimentation by forming withdrawal basins due to a combination of localized loading and structural extension (Smith *et al.* 1993; Bishop 1996; Matthews *et al.* 2007). Pod development was active in the study area throughout the Triassic and provided

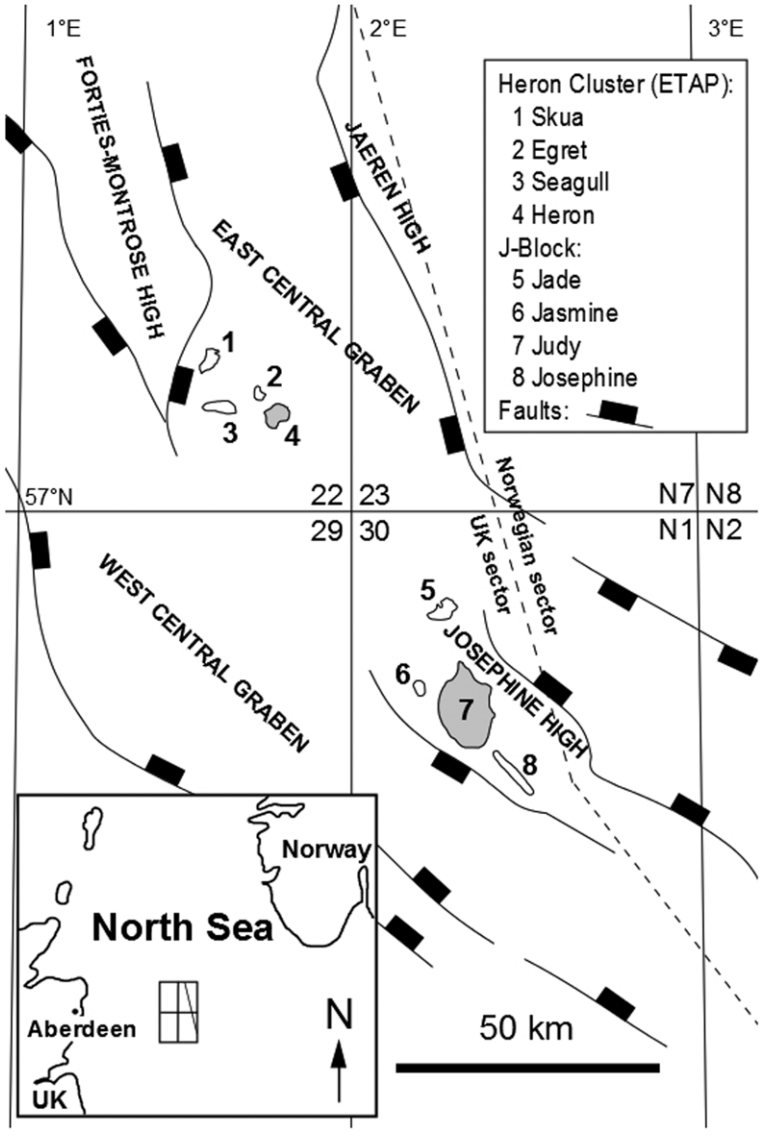

Fig. 1. Location map showing major structural elements of the Central Graben, North Sea (East Central Graben, Forties-Montrose High, Josephine High and West Central Graben) and some Triassic targets within the UK quadrant 22 (Heron Cluster) and UK quadrant 30 (J-Block). The wells chosen are from fields shaded grey.

localized depocentres for the south-easterly flowing Skagerrak fluvial system. The pods were largely responsible for the preservation of the Skagerrak Formation in the study area. However, the salt pods do create facies variability between intra- and inter-pod deposits and influenced reservoir thickness and diagenetic cementation (Nguyen *et al.* 2013).

The stratigraphic nomenclature of the Triassic for the Central Graben was defined by Goldsmith *et al.* (1995), based on detailed biostratigraphic and lithostratigraphic correlation. The Central Graben Triassic succession consists of sediments belonging to the Early Triassic Smith Bank Formation and the Middle to Late Triassic Skagerrak Formation (Fig. 2). The Triassic Skagerrak Formation is subdivided into three sand-dominated units (Judy, Joanne and Josephine) and three mud-dominated units (Julius, Jonathan and Joshua). The sand-dominated units include sheetflood deposits and multistorey

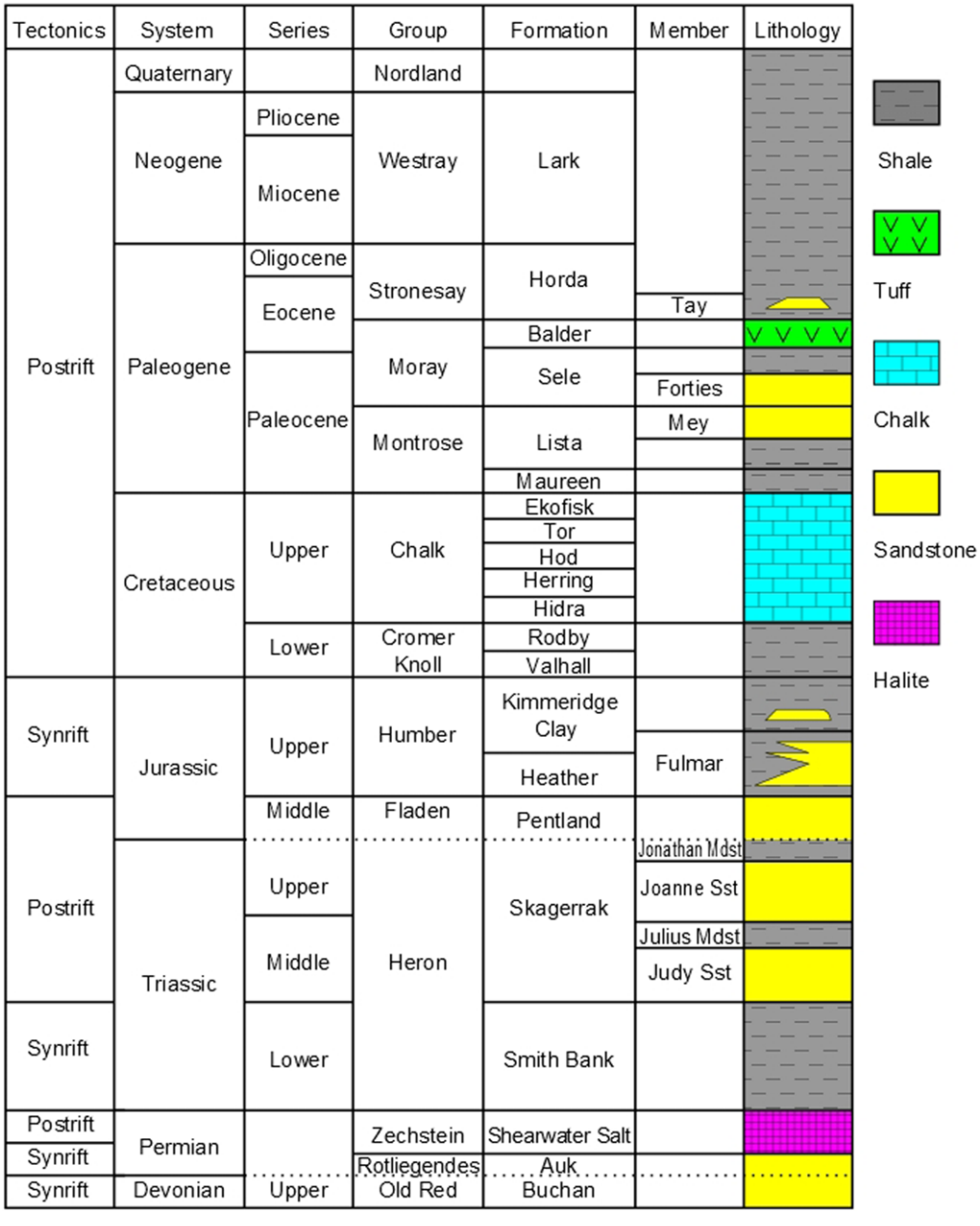

Fig. 2. Regional stratigraphy of the Central Graben, North Sea. North Sea stratigraphic nomenclature based on Knox & Cordey (1992).

stacked channel sandbodies (Goldsmith *et al.* 1995; McKie & Audretsch 2005), whereas the mud-dominated units include a variation of non-marine, basin-wide floodplain and playa deposits. The thick and laterally extensive mud-dominated units provide the main correlative units for the Triassic Skagerrak in the Central Graben (McKie & Audretsch 2005).

The resultant Triassic stratigraphy in UK quadrants 22 and 30 is incompletely preserved due

to deep erosion during the Middle and Late Jurassic (Erratt *et al.* 1999). In the J-Block area, the Skagerrak Formation includes both Judy and Joanne Sandstone Members, whereas in the Heron Cluster area only the Judy Sandstone Member is preserved (Figs 1 & 2).

Methodology

Sampling

Core samples and thin sections from six wells in the Judy field (30/7a-7; 30/7a-8; 30/7a-9; 30/7a-11Z; 30/7a-P3; 30/13-5) and one well in the Heron field (22/29-5) have been examined in this study. The 74 Judy core samples were chosen from 3400 to 4000 mbsf to cover the main reservoir fluvial facies for the Joanne and Judy Sandstone Members (Fig. 2). The 136 Heron core samples were chosen from 4300 to 4500 mbsf to cover the main reservoir facies of the Judy Sandstone Member (Fig. 2).

Petrography

Optical porosity, grain size and the fraction of chlorite-coated grains were measured for this study. Optical porosity was measured by using the jPOR digital image analysis technique (Grove & Jerram 2011) on blue epoxy-impregnated thin sections. Grain-size distribution was analysed by using the Leica QWin (V. 3.5.0) software on thin section micrographs and the fraction of chlorite-coated grains was measured by point counting with 300 counts per thin section. The resulting data were used to select samples for additional petrographic analysis (i.e. intergranular volume (IGV) (Paxton *et al.* 2002), total cement volume, porosity loss by mechanical compaction (COPL) and porosity loss by cementation (CEPL) (Lundegard 1992). The samples for further petrographic analysis were also selected by grain size (0.1–0.15 mm) to exclude the effects of grain size on the porosity and intergranular volumes. The intergranular volume and the total cement volume were measured by point counting with 300 counts per thin section.

All thin sections were highly polished to 30 μm and coated with carbon prior to analysis by a Hitachi SU-70 field emission scanning electron microscope (SEM) equipped with an energy-dispersive detector (EDS). Scanning electron microscope analyses of thin sections and bulk rock samples were conducted at acceleration voltages of 5–20 kV with beam currents of 1 and 0.6 nA, respectively. Point analyses had an average duration of 2 min, whereas line analyses were dependent on length. The SEM–EDS assembly was used for rapid identification of chemical species and orientation on the sample.

One-dimensional basin modelling

One-dimensional burial modelling was used to model pore pressure, as it provides a good insight into the pore pressure built up by disequilibrium compaction and pore fluid expansion due to increasing temperatures. Nevertheless one-dimensional models are limited in terms of integrating pore pressure mechanisms such as fluid flow, diagenetic processes, and hydrocarbon charging or gas generation. The one-dimensional burial history simulations were undertaken using Schlumberger's PetroMod (v. 2012.2) software. The software is based on a forward-modelling approach to calculate the geological evolution of a basin and burial history. The one-dimensional burial models are set up from the present-day well stratigraphy, well log lithology and lithological description of the modelled units (Table 1). To create optimum one-dimensional models, it is essential have accurate palaeoheat flow models. Several heat flow models have been published for the North Sea and especially for the Central Graben and can be subdivided into two main types: constant heat flow models (e.g. Schneider & Wolf 2000) and thermal upwelling models (e.g. Swarbrick *et al.* 2000; Carr 2003; di Primio & Neumann 2008). In this study we used the palaeo-basement heat flow and palaeo-surface temperature history published by Swarbrick *et al.* (2000). These data provide the best fit to the rifting events of the Central Graben, North Sea. The lithological unit types used in this model are mainly PetroMod default lithology types or mixed default lithology types based on well log descriptions and core analysis reports for the Central Graben lithologies. The only exceptions are the modelled Chalk units, which were modified to match the specific characteristics of the North Sea non-reservoir chalk (Mallon & Swarbrick 2002; Mallon *et al.* 2005; Swarbrick *et al.* 2010).

Petrography and diagenesis of the Skagerrak Formation

The present-day reservoir quality of the Triassic Skagerrak samples is a cumulative product of depositional attributes, mechanical compaction and diagenesis during early and later stages of burial.

Grain size and porosity distribution

The 136 investigated samples of the Heron field show a wide range of porosity from below 1% up to a maximum of 31% (Fig. 3). The porosity distribution shows a very high fraction (>90% of the samples) at porosities below 15%, which leads to an average porosity of 3.9% for the Heron field

Table 1. *Model parameters, with estimated depositional periods in millions of years, layer thicknesses in metres, modelled erosion (E) in metres and lithology (Sh: Shale and Sst: Sandstone) for the Heron and Judy 1D burial history models*

Time				Heron			Judy		
Start [Ma]	End [Ma]	Formation	Subformation	Thickness [m]	E [m]	Lithology	Thickness [m]	E [m]	Lithology
53	0	Hordaland							
10	0		Hordaland 2	1407		Shale	1424		Shale
53	10		Hordaland 1	1396		Shale	1357		Shale
54.1	53	Tay Sand		15		Silty sh			
54.3	54.1	Balder		18		Shale	17		Silty sh
54.8	54.3	Sele				Shale	54		Silty sh
54.45	54.3		Upper Sele	7					
54.65	54.45		Rogerland	16					
54.8	54.65		Lower Sele	8					
56.1	54.8	Forties		187		Sst			
58.5	56.1	Lista		49		Silty sh	16		Shale
60	58.5	Andrew		51		Silt			
59	58.5		Andrew Clay				18		Shale
59.1	59		Andrew Sand				8		Sst
59.7	59.1		Andrew Silt				50		Silty sh
60	59.7		Andrew Clay				13		Shale
61	60	Maureen		82		Marl			
60.5	60		Maureen Melange				37		Sst
61	60.5		Maureen Marl				55		Marl
65	61	Ekofisk		94		Chalk	28		Chalk
74	65	Tor		459		Chalk	226	0	Chalk
93.5	74	Hod		335		Chalk	154		Chalk
98.9	93.5	Herring		9		Chalk			
136.5	127	Valhall					22	0	Sandy shale
129.5	127		Upper Valhall	43	15	Marl			
136.5	129.5		Lower Valhall	20		Marl			
160	144	Upper Jurassic		0	50	Sandy shale	0	50	Sandy shale
180	160	Mid Jurassic		0	20	Shale	0	20	Shale
188	184	Lias					3		Shale
205.7	195	Lower Jurassic		0	150	Sst	0	150	Sst
241.7	205.7	Skagerrak							
211	205.7		Joshua	0	50	Silty shale	0	50	Silty shale
214	211		Josephine	0	100	70% sst 30% shale	0	100	70% sst 30% shale
220.7	214		Jonathan	0	40	Silty shale	38		Silty shale
234.3	220.7		Joanne	23	375	70% sst 30% shale	469		70% sst 30% shale
237	234.3		Julius	41		Silty shale	140		Silty shale
241.7	237		Judy	339		70% sst 30% shale	385		70% sst 30% shale
251.2	241.7	Smith Bank		200		Silty shale	200		Silty shale
259	251.2	Zechstein		208		Salt	208		Salt

Sst, sandstone.

samples. The grain sizes vary from coarse silt to medium-grained sand, with the majority of the samples between very fine and fine grained (Fig. 4), and an average grain size of 0.147 mm. The Heron field samples have a narrow range of compositions with most in the range of arkosic to lithic–arkosic arenites (McKie *et al.* 2010; Nguyen *et al.* 2013).

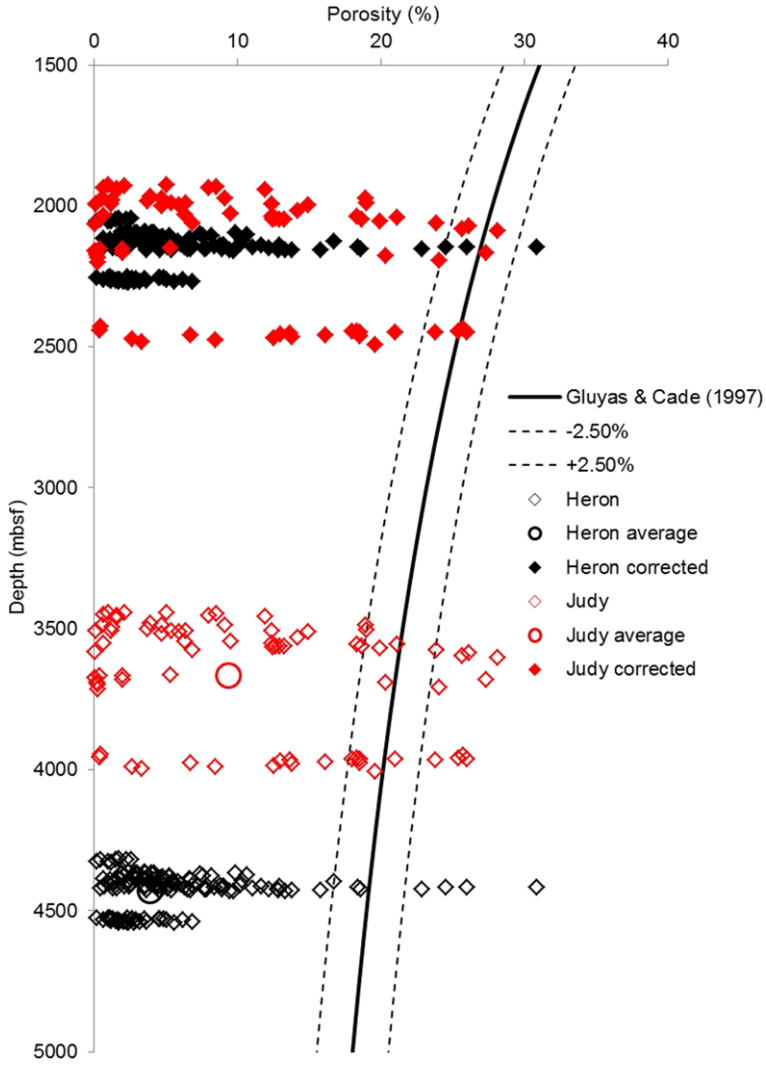

Fig. 3. Porosity–depth measurements with original sample depths and the corrected sample depths and porosity–depth relationship. After Gluyas & Cade (1997).

The 74 samples from the six Judy field wells show porosities ranging from below 1% up to a maximum of 28% (Fig. 3). The porosity distribution of the Judy field samples shows two-thirds of the porosities below 15% porosity, which leads to an average porosity of 9.4%. The grain size distribution of the Judy field samples range from coarse silt to medium-grained sand, with the majority of the investigated samples being very fine to fine grained (Fig. 4), and an average grain size of 0.131 mm. Compositionally, the Judy field samples show a similar narrow range from arkosic to lithic–arkosic arenites (McKie *et al.* 2010; Nguyen *et al.* 2013).

Mechanical compaction

Mechanical compaction in sandstones can be identified by bending of weak grains (mica), deformed soft lithic grains, local fracturing and dissolution at grain contacts, which produces concavo–convex or sutured/stylolitic grain contacts.

The Heron field samples show features of a low degree of mechanical compaction such as deformation of soft lithic grains, slight bending of micas and concavo–convex grain contacts of some detrital quartz (4391 m; Fig. 5a). In contrast, the Judy field samples show no mechanical compaction features,

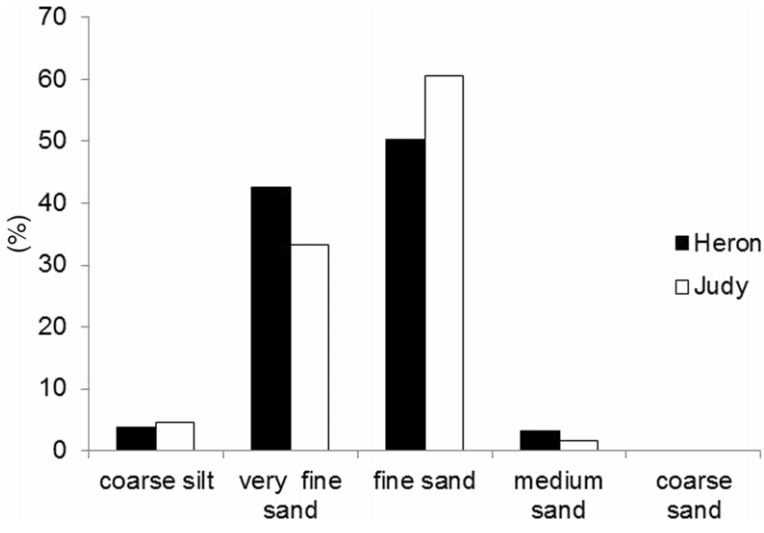

Fig. 4. Grain size distribution for samples from the Heron (136) and the Judy (74) fields.

and the samples appear to be undercompacted at their current depth of burial (3558 m; Fig. 5b).

Diagenetic cement and grain coatings

The diagenesis of the Skagerrak Formation has been the subject of a number of research papers (e.g. Smith *et al.* 1993; Weibel 1998; Kape *et al.* 2010; Nguyen *et al.* 2013). These have highlighted the complex diagenetic history of the sandstone reservoirs and how grain size and facies play an important role. The main diagenetic cements recognized include quartz, localized carbonate (ferroan dolomite) and feldspar, and early precipitates of halite

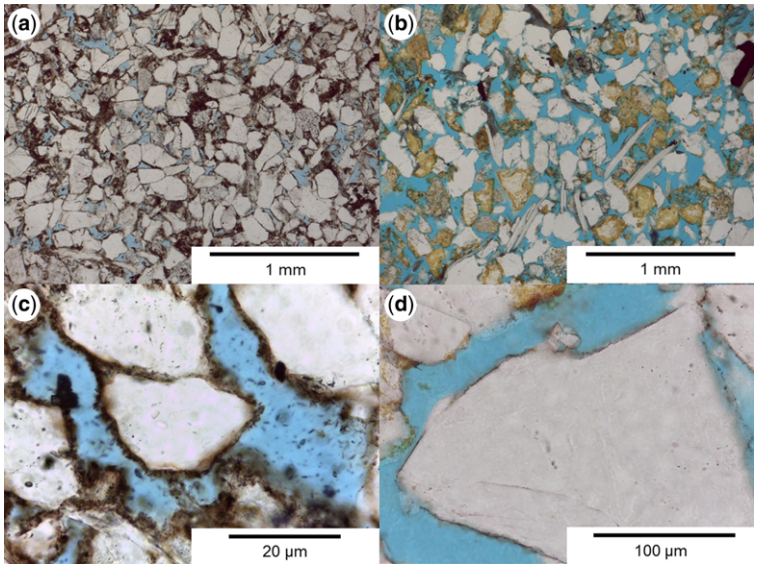

Fig. 5. Micrographs from (**a**) the Heron field sample at 4391 m with mechanical compaction features (e.g. bended mica grain, concavo-convex grain); (**b**) the Judy field at 3558 m with no mechanical compaction features and high porosity; (**c**) the Heron field at 4393 m with thick and complete covering chlorite coatings, and (**d**) the Judy field at 3548 m with thin, partly covering chlorite coatings.

cement as identified by Nguyen *et al.* (2013). Detrital grain coatings such as chlorite are common and their presence has been correlated with low volumes of quartz cement. The major cement types and detrital grain clay coatings important for reservoir quality in this study are discussed in more detail below.

Quartz cements

The quartz cements recognized in this study are common as two diagenetic stages: either an earlier microquartz overgrowth, below and in between the chlorite grain coatings, or a later macroquartz overgrowth, present at non-chlorite coated grain surfaces or at breaks in the grain coatings. The term microquartz overgrowth is used here for polycrystalline growth patterns of individual micro-sized (1–5 μm in length) quartz crystals, which are in optical continuity or discontinuity with the detrital quartz grain. In comparison the macroquartz overgrowth is defined as syntaxial quartz overgrowth larger than 20 μm in optical continuity with the detrital quartz grain.

Minor amounts of macroquartz (≤1% bulk volume) are recognized in the Heron Cluster dataset and typically are only present at rare gaps or breaks in the chlorite grain coatings. Microquartz is more common and can be observed between the detrital quartz grains and the well-developed chlorite grain coatings. The microquartz overgrowths tend to fill small cavities in the detrital quartz grain surface and infill the void space between the detrital surface and the chlorite crystals. Hydrothermal experiments on fluvial–deltaic sediments at similar temperatures to those found in the Skagerrak Formation (~160°C) have identified that quartz cement can fill significant microporosity within diagenetic chlorite coats, potentially affecting mechanical and petrophysical rock properties (Ajdukiewicz & Larese 2012).

Quartz cements play a more significant role in the Judy field datasets, where macroquartz overgrowths commonly occur in all wells but are particularly common in the deepest wells (Fig. 5b). In the deeper-buried sandstones macroquartz overgrowths commonly occur where there are breaks in the thinner, less-well-developed chlorite coatings. Furthermore, small syntaxial quartz overgrowths were also observed on grain surfaces beneath chlorite grain coatings.

Chlorite grain coatings and cement. Detailed SEM analysis identified that chlorite is the most common clay grain coating for all datasets in this study. Chlorite coatings represent over 95% of the clay mineral coatings recognized but frequently occur in close association with illite and mixed-layer chlorite–smectite or illite–smectite. A complex structural pattern for the chlorite grain coatings is observed in all cases, regardless of coating thickness. A root zone (Pittman *et al.* 1992; Ehrenberg 1993) with platey crystals parallel to the surface of the detrital grain is superseded by well-defined platey to curly crystals that grew perpendicular to the detrital surface (Fig. 6a).

The Heron field samples show in general a high fraction (80–100%) of chlorite-coated grains (Fig. 7). Grain coatings are very well developed and range from 1 μm to >20 μm thick, with an average of 11 μm. The coatings are generally absent at grain–grain contacts, but show a very high detrital grain surface coverage of around 95% (Fig. 5c).

The fraction of the chlorite-coated grains in the Judy field samples is more variable, ranging between 10% and 70% (Fig. 7). Chlorite grain coatings vary in thickness from 1–15 μm, with average thicknesses of ~7 μm. The coatings are absent at grain–grain contacts and commonly incomplete in their surface coverage of detrital quartz grains (Fig. 5d). Furthermore, there appears to be a direct relationship between the measured porosity of the sandstone datasets and the fractions of chlorite-coated grains (Fig. 8). The Heron dataset

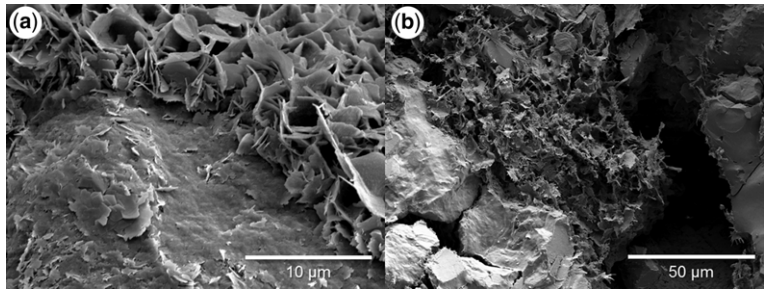

Fig. 6. SEM images from (**a**) the Heron field sample at 4393 m with a clay coating root zone parallel to the detrital grain surface and a second layer of well-defined chlorite crystals oriented perpendicular to the detrital surface, and (**b**) the Heron field sample at 4417 m with a pore-filling clay mixture of chlorite and illite.

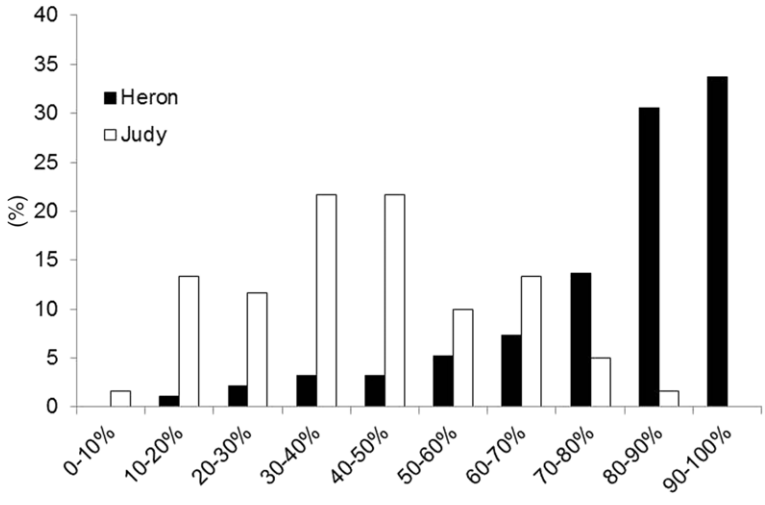

Fig. 7. Fraction of chlorite-coated detrital grains per 300 counts for the 136 Heron samples and the 74 Judy samples.

demonstrates a consistently lower porosity (<15%) for lower fractions of coated grains (<15%), whereas high porosities of up to 30% for higher fractions (>50%) of chlorite-coated grains are common. The Judy dataset does not illustrate such a close relationship between porosity and percentage of coated grains (Fig. 8).

Authigenic chlorite cements are the most important and effective grain coating in terms of limiting early extensive quartz cementation in the Skagerrak sandstones. However, pore-filling chlorite, illite and chlorite–illite mixes commonly occur in the sandstones from the Heron samples. The pore-filling cements comprise small chlorite plates that are orientated parallel and arranged with a denser packing than seen for grain coatings (Fig. 6b). Chlorite-coated grains are locally covered by pore-filling chlorite cements. They represent between 10% and 15% of the bulk rock sample and can fill up to 50% of the remaining intergranular volume (Fig. 5a). In the Skagerrak sandstones from the Judy field authigenic pore-filling chlorite is rarely

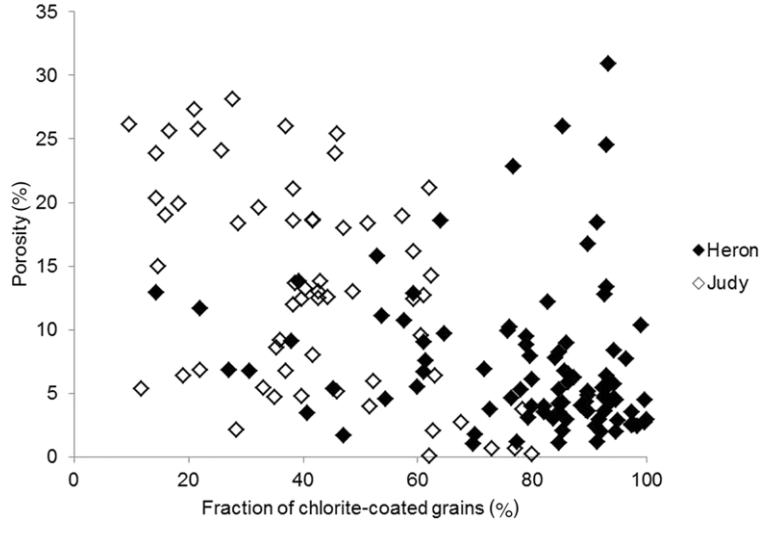

Fig. 8. Measured porosity v. fraction of chlorite-coated detrital grains for the Heron and the Judy samples.

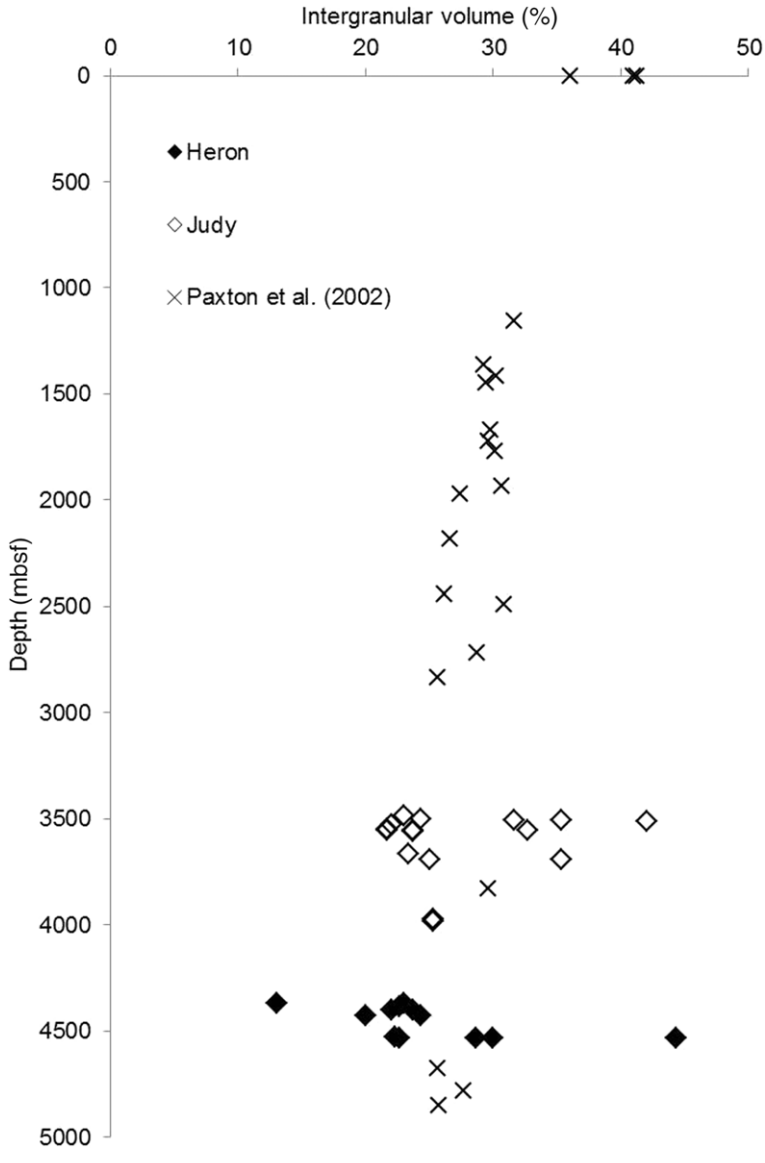

Fig. 9. Intergranular volume (IGV) v. depth for the Heron samples and the Judy samples, with observed reference IGV from Paxton *et al.* (2002).

identified (<5%), (Fig. 5b). This may in part reflect the less-well-developed chlorite grain coatings and occurrence in the Judy compared with the Heron fields (McKie *et al.* 2010; Nguyen *et al.* 2013).

K-feldspar dissolution

K-feldspar dissolution and alteration can be observed in both sample sets. K-feldspar dissolution occurs generally at a late burial stage, after the precipitation of the chlorite grain coating. This is indicated by chlorite grain coatings that preserve the original shape of the partly or fully dissolved K-feldspar grain.

K-feldspar dissolution can be observed in the Heron field samples, but is less common than in the Judy field samples (Fig. 5). Partial dissolution of detrital K-feldspar grains is observed from depths greater than 3200 m (Fig. 5).

Table 2. *Total cement volume (C), measured porosity (P_o), minus-cement porosity (P_{mc}) or intergranular volume (IGV), porosity-loss by mechanical compaction (COPL) and porosity-loss by cementation (CEPL) all in % for the Heron and Judy sample sets*

Field	C [%]	P_o [%]	P_{mc}/IGV [%]	COPL [%]	CEPL [%]
Heron	17.00	6.00	23.00	28.57	12.14
	11.00	2.00	13.00	36.78	6.95
	15.00	7.67	22.67	28.88	10.67
	11.67	10.33	22.00	29.49	8.23
	18.00	5.67	23.67	27.95	12.97
	8.33	11.67	20.00	31.25	5.73
	14.33	10.00	24.33	27.31	10.42
	21.00	1.33	22.33	29.18	14.87
	19.67	3.00	22.67	28.88	13.99
	28.67	1.33	30.00	21.43	22.52
	37.00	7.33	44.33	1.20	36.56
	28.67	0	28.67	22.90	22.10
Average	19.19	5.53	24.72	26.15	14.76
Judy	11.00	12.00	23.00	28.57	7.86
	5.00	19.33	24.33	27.31	3.63
	20.33	11.33	31.67	19.51	16.37
	35.67	6.33	42.00	5.17	33.82
	5.67	16.00	21.67	29.79	3.98
	15.67	17.00	32.67	18.32	12.80
	13.00	10.33	23.33	28.26	9.33
	7.33	17.67	25.00	26.67	5.38
	13.00	22.33	35.33	14.95	11.06
	20.00	15.33	35.33	14.95	17.01
	8.67	13.33	22.00	29.49	6.11
	15.67	6.00	21.67	29.79	11.00
	4.33	19.33	23.67	27.95	3.12
	5.67	18.00	23.67	27.95	4.08
	10.00	18.67	28.67	22.90	7.71
	4.00	15.67	19.67	31.54	2.74
	10.00	15.33	25.33	26.34	7.37
	14.00	11.33	25.33	26.34	10.31
Average	12.17	14.74	26.91	24.21	9.65

Intergranular volume and total cement volume

Total cement and IGV measurements were undertaken on samples with grain sizes between 0.1 and 0.15 mm to reduce grain size variations. The IGV, or minus-cement porosity, is the sum of intergranular pore space, intergranular cement and depositional matrix (Paxton *et al.* 2002). The results of the IGV measurements show wide variations for both sample sets. The Heron field IGVs vary from 13% to 44%, with the majority between 20% and 30% and a mean of 22.8%. The Judy field IGVs range between 20% and 42%. The Judy field IGVs plot in two clusters, between 20–25% and 31–42%, with an overall mean of 24.6% (Fig. 9). The total cement volume represents the volume of all pore-filling diagenetic cements, including quartz, chlorite, illite and other clay mineral cements. The total cement volume is used to calculate the porosity loss by mechanical compaction and by cementation (Lundegard 1992). The total cement volume varies for the Heron samples from 8% up to 37%, with an average of 19%. The Judy field samples show total cement volumes from 4% to 35%, with a lower average of 12% (Table 2). The measured total cement volume (C) can be used to calculate the porosity-losses caused by compaction (COPL) and cementation (CEPL) using the following equations after Lundegard (1992):

$$\mathrm{COPL} = P_i - \left(\frac{(100 - P_i)P_{mc}}{100 - P_{mc}}\right) \quad (1)$$

$$\mathrm{CEPL} = (P_i - \mathrm{COPL})\left(\frac{C}{P_{mc}}\right) \quad (2)$$

where P_i is the initial or depositional porosity and P_{mc} is the IGV or minus-cement porosity calculated from by subtracting the total cement volume, C from the total optical porosity, P_o (Table 2). The calculated COPL and CEPL are only accurate if three conditions are met. First, the assumed initial porosity P_i is correct. Second, the amount of cement derived by local grain dissolution is negligible or known. And third, the amount of framework mass exported by grain dissolution is negligible or known (Lundegard 1992). The initial or depositional porosity assumed for the Skagerrak sandstones samples is 45% (Lundegard 1992). The COPL–CEPL results show porosity loss for both sample sets was predominantly by mechanical compaction (Fig. 10), with averages of 26% and 24% for the Heron and the Judy sample sets, respectively. Furthermore, the results show a CEPL of 15% for the Heron sample set, 5% higher CEPL than for the Judy sample set (Table 2).

Burial history modelling

The one-dimensional burial history models show that the Triassic Skagerrak units are at maximum burial depth and maximum temperature at present day (Fig. 11). The Skagerrak Formation experienced a long shallow burial phase (<1800 mbsf) between deposition and 80 Ma, followed by a phase of rapid burial to their present maximum burial depths. During this rapid burial phase, overpressure started to build up at around 80 Ma ago in the Heron field (Fig. 12a) and at around 70 Ma ago in the Judy field (Fig. 12b). The onset of overpressure in both fields occurred during shallow burial at around 650 m burial depth for the Heron field (Fig. 12a) and around 500 m burial depth for the Judy field (Fig. 12b). The pore fluid pressure

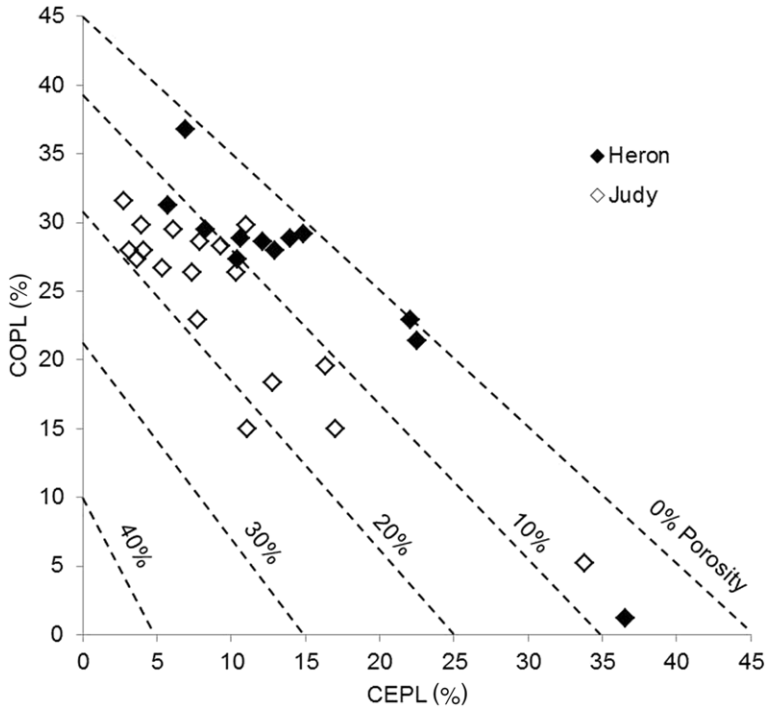

Fig. 10. Mechanical compaction (COPL) and cementational (CEPL) porosity loss for the Heron and the Judy sample set. After Lundegard (1992).

increased during ongoing burial to a present-day maximum for the whole study area. The increase in pore fluid pressure causes a reduction in vertical effective stress with ongoing burial (Fig. 12). The present-day pore fluid pressures for both wells increase downwards through the Chalk units (Ekofisk, Tor and Hod formations) to the Triassic Skagerrak units (Fig. 13). In this model, the only mechanisms for generating overpressure that have been taken into account are disequilibrium compaction and fluid expansion, which explains the lower-than-measured pore fluid pressures for the Heron field and the Judy field. Nevertheless, the models for the Judy field, based on the well 30/7a-9 (Fig. 13a), and the Heron field, based on the well 22/29-5 (Fig. 13b), show pore fluid pressure trends in agreement with measured trends from repeat formation tester (RFT) pressure data.

Overpressure-depth correction

The modelled pore fluid overpressure, generated by disequilibrium compaction, can be used to estimate the equivalent depth where the measured porosity would be found on the normal compaction curve, i.e. if the pore pressure were hydrostatic. For the normal compaction curve, we used the porosity–depth relationship of Gluyas & Cade (1997), which is based on experimental data from laboratory compaction experiments for uncemented sandstones under hydrostatic burial:

$$\varphi = 50 \exp\left(\frac{-10^{-3}z}{2.4 + 5 \cdot 10^{-4}z}\right) \tag{3}$$

where φ is porosity expressed as a percentage and z is depth in metres. The depth and the rate of mechanical compaction are corrected by scaling the porosity to vertical effective stress, rather than to depth (Gluyas & Cade 1997). The compaction-only porosity–depth relationship is:

$$z' = z - \left(\frac{u}{(\rho_r - \rho_w)g\left(1 - \varphi_{\varepsilon\sum}\right)}\right) \tag{4}$$

where z' is the equivalent depth in metres, z is the depth in metres, u the overpressure in pascals, ρ_r is the rock density in kilograms per cubic metre (typically 2650 kg m^{-3}), ρ_w is the water density in kilograms per cubic metre (typically 1050 kg m^{-3}), g is the gravity in metres per second squared (typically 9.8 m s^{-2}), and $\varphi_{\varepsilon\Sigma}$ is the average

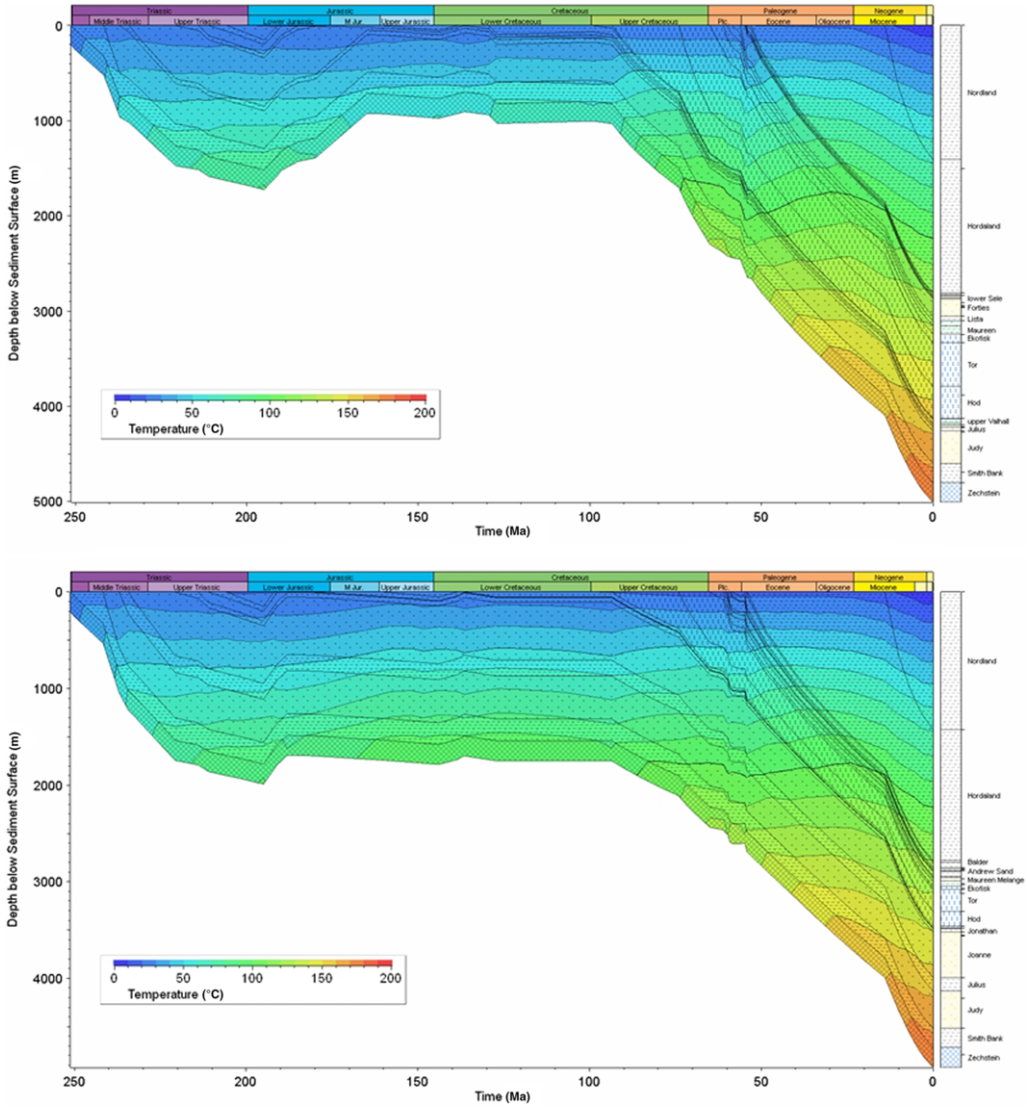

Fig. 11. 1D burial temperature plot for the Heron well (22/29-5) (top) and the Judy well (30/7a-9) (bottom) with the associated stratigraphic columns.

porosity of the overburden expressed as a fraction (typically = 0.2). The corrected depths for the Heron field samples are around 2200 m shallower, corrected from ~4400 m depth to ~2200 m depth (Fig. 3). The corrected depths for the Judy field samples are around 1500 m shallower, corrected from ~3500 to ~2000 m depth (Fig. 3). The high porosities of 25–30% in the Skagerrak sandstones, previously considered anomalous, are within the range of the porosity–depth relationship introduced by Gluyas & Cade (1997) at their corrected depths.

Discussion

Interpretation and diagenetic development

All of the observed petrographic features can be linked into a relative sequence for both reservoirs. The eodiagenetic, dolomitic cements were precipitated early during the initial phase of mechanical compaction and decrease of IGV. This is indicated by high IGVs (close to depositional IGV), in the dolomitic cemented samples in both samples sets. The dolomite cement is likely to be sourced from

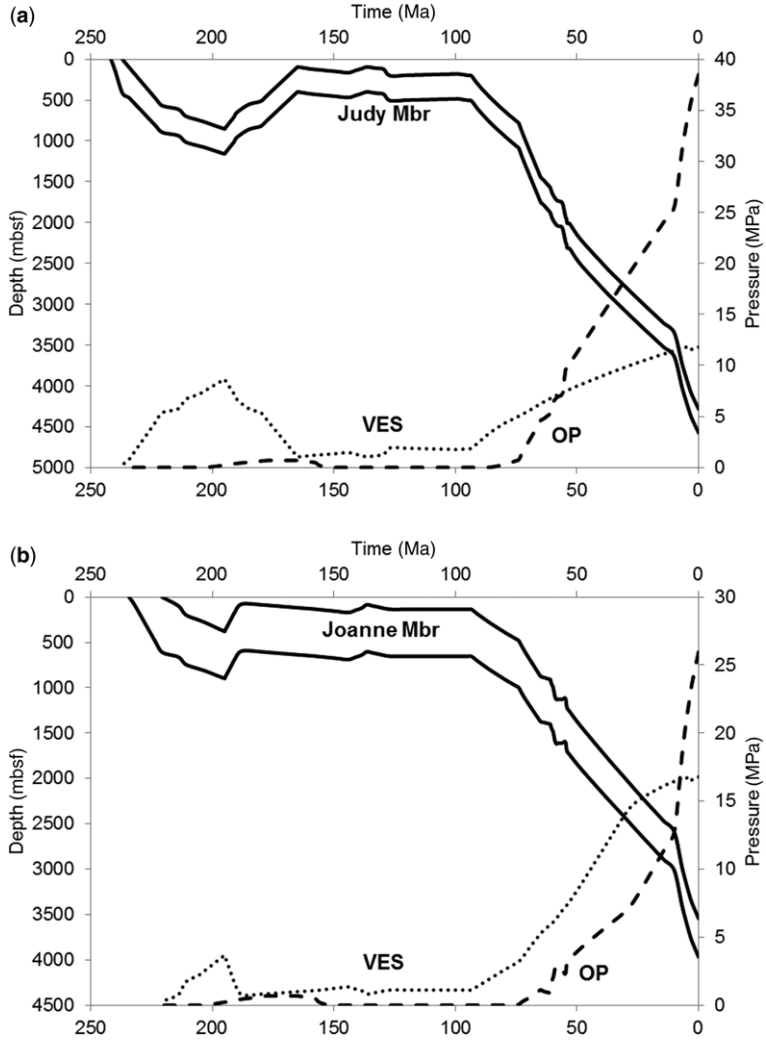

Fig. 12. Burial history (solid lines), pore fluid overpressure (OP; dashed lines) and vertical effective stress (VES; dotted lines) development for (**a**) the Judy Sandstone Member, the uppermost succession within the Skagerrak Formation in the Heron well (22/29-5) and (**b**) the Joanne Sandstone Member, the uppermost succession within the Skagerrak Formation in the Judy well (30/7a-9).

reworked calcrete or dolocrete fragments (McKie & Audretsch 2005); this is indicated by the association of the dolomitic cements with slightly deformed clay clasts. Mechanical compaction had the strongest impact during shallow burial (<2500 m), despite the shallow onset of the pore fluid overpressure which reduces the VES and hence reduces the effects of mechanical compaction. The dolomitic cements were followed by the early microquartz overgrowth, which is proven by the lack of microquartz on detrital grains surrounded by dolomitic cement. The following phase of authigenic grain coating with chlorite is probably the most important diagenetic phase for the Heron field and the Judy field. The authigenic chlorite covers the earlier microquartz on the detrital quartz grains. The authigenic chlorite coatings possibly developed during early mesodiagenesis, at temperatures of 60–100°C. The chlorite probably originates from precursor clay minerals such as smectite, berthierine and kaolinite (Grigsby 2001; Worden & Morad 2003; Berger *et al.* 2009) or the dissolution and reprecipitation of syndepositional chlorite (Anjos *et al.* 2003). These authigenic chlorite grain coatings inhibited a further stage of quartz cementation above temperatures of 70°C (Worden & Morad

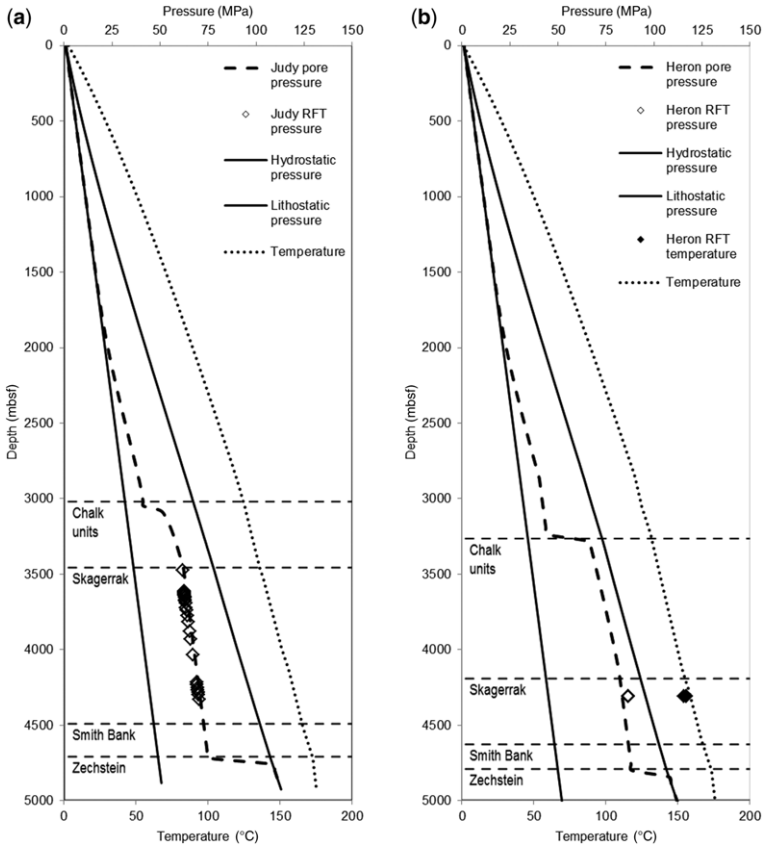

Fig. 13. Modelled formation pressures caused by disequilibrium compaction with hydrostatic pressure, lithostatic pressure and formation temperature, measured RFT pressure and temperature data for (**a**) the Judy field (30/7a-9) and (**b**) the Heron field (22/29-5). Pore fluid pressure can exceed 80 MPa at depths of between 4000 and 5000 mbsf for both wells.

2000) in the Heron field and partly inhibit it in the Judy field. The later stage macroquartz cement is present on the non-covered detrital quartz grain surfaces. Due to the incompleteness of the authigenic coatings the amount of macroquartz cement is higher in the Judy field sample. Deposition of the chlorite grain coats was also followed by a stage of extensive feldspar dissolution in the Judy field, less prominent in the Heron field. The feldspar dissolution phase occurred with, or was closely followed by, a phase of secondary precipitation of pore-filling chlorite and illite, which is likely to have been synchronous with the feldspar alteration and dissolution (Worden & Morad 2003).

Role played by chlorite grain coatings

The occurrence of quartz overgrowths is closely related to chlorite grain coatings (Pittman & Lumsden 1968; Dixon *et al.* 1989; Pittman *et al.* 1992; Ehrenberg 1993; Anjos *et al.* 2003; Berger *et al.* 2009; Ajdukiewicz & Lander 2010; Bahlis & De Ros 2013); therefore the role played by the chlorite grain coatings is important in terms of maintaining primary porosity. This role could not be more different in the two investigated reservoirs.

The Heron field chlorite coatings are thickly developed and, in most cases, cover the detrital quartz grain surfaces completely (Fig. 5a, c). The full coverage of the robust chlorite grain coatings, with their well-developed root zone and their second layer of well-defined perpendicular oriented crystals, seems to be the key in inhibiting extensive macroquartz cement overgrowth at temperatures above 70°C (Worden & Morad 2000). Similar effects on quartz overgrowth have been described by Dixon *et al.* (1989), Pittman *et al.* (1992), Ehrenberg (1993), Anjos *et al.* (2003), Berger *et al.* (2009), Bahlis & De Ros (2013) and Ajdukiewicz & Lander (2010) for other formations with thick and fully

covering chlorite grain coatings. The inhibition of quartz cement is potentially the cause for the correlation between porosity and the fraction of coated grains in the Heron field samples (Fig. 8).

The Judy field samples show thin chlorite grain coatings with major gaps and macroquartz overgrowths (Fig. 5d). The impact of grain coatings on the maintenance of porosity is highly dependent on their completeness (Ajdukiewicz & Lander 2010; Ajdukiewicz & Larese 2012). Despite their incomplete coverage, the Judy field coatings are still inhibiting extensive quartz cement precipitation on around 80% of the detrital surfaces. The main nucleation points for the quartz overgrowths are the non-covered gap areas of the detrital quartz grain surfaces where macroquartz overgrowth can be observed (Fig. 5d). Nevertheless, macroquartz overgrowth is less extensive than expected due to the incomplete coverage in the Judy field samples. This could be due to a low concentration of dissolved silica in the pore fluid. The Judy reservoir experienced pore fluid overpressure at relatively shallow depths, which leads to a semi-closed system, low VES, less mechanical compaction and less pressure dissolution at grain contacts. Therefore less silica is dissolved in the reservoir and, due to the pore fluid overpressure, lateral transfer of pore fluid is less likely. This could be a possible explanation for a lower ratio of dissolved silica in the Judy field reservoir.

Nevertheless, it has been reported that thick and extensive chlorite coatings could reduce the reservoir quality by decreasing the porosity and, probably more significantly, the permeability, by bridging and closing of pore throats (Anjos *et al.* 2003; Bahlis & De Ros 2013). Therefore it seems that the thickly developed chlorite coatings in the Heron reservoir have also had contrary impacts on the porosity by bridging the gap between one grain coating to another across open pore space, and filling that pore space with chlorite cement. Some of the thick chlorite coatings actually have a net effect of decreasing the overall porosity, and also reduce the permeability of the reservoir sandstones instead of increasing it. This observation is confirmed by the 5% higher CEPL in the Heron samples compared with the Judy samples (Fig. 10). This porosity reduction is not caused by quartz cementation but by bridging and pore-filling chlorite.

Effect of pore fluid overpressure on porosity preservation

The positive effect of pore fluid pressure on the maintenance of primary porosity has been well known since Terzaghi's introduction of the effective stress concept: overpressured reservoirs are often associated with higher porosities. However, a combination of the magnitude and timing of onset of overpressure needs to be considered in reservoirs with enhanced primary porosity preservation. Pore fluid overpressure can arrest and slow down mechanical compaction, but cannot increase porosity. Therefore the timing of the onset of overpressure is the crucial factor in maintaining primary porosity by overpressure to depth. Furthermore, overpressured reservoirs are often closed or at least semi-closed systems with minimal or no external fluid exchange, which allows them to evolve in their own fluids (Jeans 1994). The exclusion of external sources reduces the number of possible cementational processes in the reservoir and allows better predictions of these processes.

The onset of overpressure in the Heron field was around 80 Ma years ago, which provides an onset burial depth of around 650 m for the investigated samples (Fig. 12a). The pore fluid overpressure then started to ramp up significantly due to the rapid burial and the massive overlaying packages. The VES on the Heron field grain framework further increased during the rapid burial of the Triassic Skagerrak units, but the rapidly increasing pore fluid overpressure reduced the rate of VES increase dramatically (Fig. 12). This slower-than-expected VES increase from the shallow burial depth of 650 m reduced the effects of mechanical compaction on the grain framework significantly. This reduced mechanical compaction can be seen in the investigated samples, where characteristics of a medium compaction state are present (slight bending of mica grains, grain contact dissolution with concavo–convex contacts), but there are no features of a high compaction state (sutured or stylolitic grain contacts and grain fracturing) (Fig. 5a) that would be expected in this deep burial stage.

The overpressure onset in the Judy field was around 70 Ma years ago, at around 500 m burial depth for the investigated samples (Fig. 12b). The pore fluid pressure started to ramp up, which led to a reduced rate of increase for the VES. The lower-than-expected VES led to less mechanical compaction in the Judy field; this can be observed in the investigated samples. There are no common mechanical compaction features such as bent mica grains, fractured grains, pressure dissolution or concavo–convex or sutured grain contacts for the Judy field samples (Fig. 5b). Consequently, greater primary porosity was maintained in the Judy field.

Nevertheless, in both case studies the overpressure only had an impact on the porosity preservation because of its shallow onset, in the case of a deeper onset most of the preserved primary porosity would have been lost due to ongoing mechanical compaction. There would have been almost no effect if overpressure onset occurred at greater

depths (>2500 mbsf), when the sandstones had become sufficiently lithified that mechanical compaction was no longer taking place (Paxton *et al.* 2002).

The porosity-preserving impact of the overpressure is shown by the overpressure–depth correction after Gluyas & Cade (1997). The anomalously high porosities for deeply buried sandstone reservoirs, above 20%, are well within the expected range of the hydrostatic porosity–depth relationship after the overpressure–depth correction (Fig. 3).

Furthermore, the IGV and the total cement measurements show that even if most of the porosity loss in both reservoir sandstones has been due to mechanical compaction (Fig. 10), the impact of pore fluid overpressure on porosity maintenance seems to have been considerable in sandstones reservoirs. However, it is not just the overpressure or the magnitude of overpressure that are important and control the VES, the depth of onset is also crucial: the shallower the onset, the greater the potential for preserving high primary porosity.

Implications for deeply buried sandstone reservoirs

Anomalously high porosities can be found in deeply buried sandstone reservoirs where a combination of porosity-preserving mechanisms have been operating. The onset of shallow (<2000 m) pore fluid overpressure reduces the VES on the grain framework and hence reduces the amount of mechanical compaction. Nevertheless, the impact of pore fluid overpressure on the precipitation of cements seems to be negligible, given that temperature and availability of dissolved material is the main driver of cementation (Walderhaug 1994; Oelkers *et al.* 1996; Osborne & Swarbrick 1999).

Therefore, clay mineral or microquartz coatings are important for inhibiting extensive quartz cementation at temperatures above 70°C (Worden & Morad 2000) during deeper burial, where porosity loss is dominated by cementation processes. The effect of grain coatings on inhibiting quartz cement growth is highest in quartz-rich sandstones with silica-rich pore fluids.

It has clearly been shown by the two Triassic Skagerrak case studies that a shallow onset of pore fluid overpressure has a high potential for preserving primary porosities to depth. However, mechanisms that inhibit extensive quartz cementation are also important for porosity preservation during deeper burial (Pittman *et al.* 1992; Jeans 1994; Ajdukiewicz & Lander 2010). Primary porosity maintained by overpressure during shallow burial can be reduced significantly by extensive quartz cementation during later burial. Therefore, a combination of shallow overpressure onset and a high fraction of grains with chlorite coatings, without the development of pore-filling chlorite, is the best possible scenario for maintaining high primary porosities to depth.

Conclusions

(1) High porosities (up to 35%) at depths of >3500 mbsf and temperatures around 150°C are found in the Triassic Skagerrak fluvial sandstones of the J-Block and the Heron Cluster fields in the Central Graben, North Sea.

(2) The rate of porosity decline with increasing burial depth has been significantly arrested by a combination of shallow overpressure development and chlorite coatings of detrital grains.

(3) Timing of overpressure development was crucial as later overpressure development would probably have resulted in poorer reservoir quality for the Skagerrak Formation sandstones. It seems that the isolated nature of the intrapod reservoir units in both areas contributed to the onset of overpressure at shallow burial depth.

(4) Authigenic chlorite coatings maintain porosity by inhibiting quartz cement overgrowth at temperatures >70°C (Worden & Morad 2000). However, the chlorite coatings also reduce porosity due to their very presence, especially when their growth bridges between detrital quartz grains and fills the intervening pore space.

(5) This research has shed light on the controls on reservoir quality in the complex fluvial sandstones of the Skagerrak Formation. It clearly identifies the need to understand the timing of overpressure generation for arresting mechanical compaction and the importance of chlorite detrital grain coatings in inhibiting quartz cement overgrowth as temperature increases during progressive burial.

(6) Compaction remains active until the present day, and its deleterious effects are only too evident where chlorite grain coatings are absent, even where the VES is very low.

The industry funded research consortium GeoPOP sponsored by BG, BP, Chevron, ConocoPhillips, DONG Energy, E.ON, ENI, Petrobras, Petronas, Statoil, Total and Tullow Oil, at Durham University is thanked for funding this research. We acknowledge support from the BGS (British Geological Survey) for access to core material from the Heron Cluster wells. We thank the Special Publications editors P. Armitage and R. Worden for their suggestions and reviewers S. Gier and P. Kukla for their constructive reviews to help improve the manuscript.

References

Aase, N. E., Bjorkum, P. A. & Nadeau, P. H. 1996. The effect of grain-coating microquartz on preservation of reservoir porosity. *AAPG Bulletin*, **80**, 1654–1673.

Ajdukiewicz, J. M. & Lander, R. H. 2010. Sandstone reservoir quality prediction: the state of the art. *AAPG Bulletin*, **94**, 1083–1091.

Ajdukiewicz, J. M. & Larese, R. E. 2012. How clay grain coats inhibit quartz cement and preserve porosity in deeply buried sandstones: observations and experiments. *AAPG Bulletin*, **96**, 2091–2119.

Ajdukiewicz, J., Nicholson, P. & Esch, W. 2010. Prediction of deep reservoir quality using early diagenetic process models in the Jurassic Norphlet Formation, Gulf of Mexico. *AAPG Bulletin*, **94**, 1189–1227.

Anjos, S., De Ros, L. & Silva, C. 2003. Chlorite authigenesis and porosity preservation in the Upper Cretaceous marine sandstones of the Santos Basin, Offshore Eastern Brazil. *In*: Worden, R. H. & Morad, S. (eds) *Clay Mineral Cements in Sandstones*. International Association of Sedimentologists Special Publications, **34**, 291–316.

Audet, D. M. & McConnell, J. D. C. 1992. Forward modelling of porosity and pore pressure evolution in sedimentary basins. *Basin Research*, **4**, 147–162.

Bahlis, A. B. & De Ros, L. F. 2013. Origin and impact of authigenic chlorite in the Upper Cretaceous sandstone reservoirs of the Santos Basin, eastern Brazil. *Petroleum Geoscience*, **19**, 185–199.

Berger, A., Gier, S. & Krois, P. 2009. Porosity-preserving chlorite cements in shallow-marine volcaniclastic sandstones: evidence from Cretaceous sandstones of the Sawan gas field, Pakistan. *AAPG Bulletin*, **93**, 595–615.

Bishop, D. J. 1996. Regional distribution and geometry of salt diapirs and supra-Zechstein Group faults in the western and central North Sea. *Marine and Petroleum Geology*, **13**, 355–364.

Bloch, S., Lander, R. H. & Bonnell, L. 2002. Anomalously high porosity and permeability in deeply buried sandstone reservoirs: origin and predictability. *AAPG Bulletin*, **86**, 301–328.

Carr, A. 2003. Thermal history model for the South Central Graben, North Sea, derived using both tectonics and maturation. *International Journal of Coal Geology*, **54**, 3–19.

Clark, J. A., Cartwright, J. A. & Stewart, S. A. 1999. Mesozoic dissolution tectonics on the West Central Shelf, UK Central North Sea. *Marine and Petroleum Geology*, **16**, 283–300, https://doi.org/10.1016/S0264-8172(98)00040-3

De Jong, M., Smith, D., Nio, S. D. & Hardy, N. 2006. Subsurface correlation of the Triassic of the UK southern Central Graben: new look at an old problem. *First Break*, **24**, 103–109.

di Primio, R. & Neumann, V. 2008. HPHT reservoir evolution: a case study from Jade and Judy fields, Central Graben, UK North Sea. *International Journal of Earth Sciences*, **97**, 1101–1114.

Dixon, S., Summers, D. & Surdam, R. 1989. Diagenesis and preservation of porosity in Norphlet Formation (Upper Jurassic), southern Alabama. *AAPG Bulletin*, **73**, 707–728.

Ehrenberg, S. N. 1993. Preservation of anomalously high porosity in deeply buried sandstones by grain-coating chlorite: examples from the Norwegian continental shelf. *AAPG*, **77**, 1260–1286.

Ehrenberg, S., Nadeau, P. & Steen, Ø. 2008. A megascale view of reservoir quality in producing sandstones from the offshore Gulf of Mexico. *AAPG Bulletin*, **92**, 145–164.

Ehrenberg, S. N., Nadeau, P. H. & Steen, O. 2009. Petroleum reservoir porosity v. depth: influence of geological age. *AAPG Bulletin*, **93**, 1281–1296.

Erratt, D., Thomas, G. & Wall, G. 1999. The evolution of the central North Sea Rift. *In*: Fleet, A. J. & Boldy, S. A. R. (eds) *Petroleum Geology of Northwest Europe: Proceedings of the 5th Conference*. Geological Society, London, 63–82.

French, M. W., Worden, R. H., Mariani, E., Larese, R. E., Mueller, R. R. & Kliewer, C. E. 2012. Microcrystalline quartz generation and the preservation of porosity in sandstones; evidence from the Upper Cretaceous of the Subhercynian Basin, Germany. *Journal of Sedimentary Research*, **82**, 422–434.

Gaarenstroom, L., Tromp, R. A. J., de Jong, M. C. & Brandenburg, A. M. 1993. Overpressures in the Central North Sea: implications for trap integrity and drilling safety. *In*: Parker, J. R. (ed.), *Petroleum Geology of Northwest Europe: Proceedings of the 4th Conference*. Geological Society, London, 1305–1313.

Giles, M. R. 1997. *Diagenesis: A Quantitative Perspective*. Kluwer Academic, Dordrecht.

Glennie, K. W. 1998. *Petroleum Geology of the North Sea: Basic Concepts and Recent Advances*. Blackwell, Oxford.

Gluyas, J. & Cade, C. A. 1997. Prediction of porosity in compacted sands. *In*: Kupecz, J. A., Gluyas, J. G. & Bloch, S. (eds) *Reservoir Quality Prediction in Sandstones and Carbonates*. American Association of Petroleum Geologists Memoir, American Association of Petroleum Geologists, Tulsa, USA, **69**, 19–27.

Goldsmith, P. J., Hudson, G. & van Veen, P. 2003. Triassic. *In*: Evans, D., Graham, C., Armour, A. & Bathurst, P. (eds) *The Millennium Atlas: Petroleum Geology of the Central and Northern North Sea*. Geological Society, London, 105–127.

Goldsmith, P. J., Rich, B. & Standring, J. 1995. Triassic correlation and stratigraphy in the south Central Graben, UK North Sea. *In*: Boldy, S. A. R. (ed.) *Permian and Triassic Rifting in Northwest Europe*. Geological Society, London, Special Publications, **91**, 123–143.

Gowers, M. B. & Sæbøe, A. 1985. On the structural evolution of the Central Trough in the Norwegian and Danish sectors of the North Sea. *Marine and Petroleum Geology*, **2**, 298–318.

Grant, N. T., Middleton, A. J. & Archer, S. 2014. Porosity trends in the Skagerrak Formation, Central Graben, UKCS: the role of compaction and pore pressure history. *AAPG Bulletin*, **98**, 1111–1143.

Grigsby, J. D. 2001. Origin and growth mechanism of authigenic chlorite in sandstones of the lower Vicksburg Formation, south Texas. *Journal of Sedimentary Research*, **71**, 27–36.

GROVE, C. & JERRAM, D. A. 2011. jPOR: an ImageJ macro to quantify total optical porosity from blue-stained thin sections. *Computers & Geosciences*, **37**, 1850–1859.

HASZELDINE, R. S., WILKINSON, M. *ET AL.* 1999. Diagenetic porosity creation in an overpressured graben. *In*: FLEET, A. J. & BOLDY, S. A. R. (eds) *Petroleum Geology of Northwest Europe: Proceedings of the 5th Conference*. Geological Society, London.

JEANS, C. 1994. Clay diagenesis, overpressure and reservoir quality: an introduction. *Clay Minerals*, **29**, 415–424.

KAPE, S., DE SOUZA, O. D., BUSHNAQ, I., HAYES, M. & TURNER, I. 2010. *Predicting Production Behaviour from Deep HPHT Triassic Reservoirs and the Impact of Sedimentary Architecture on Recovery*. Geological Society, London, Petroleum Geology Conference series, 405–417.

KNOX, R. W. O'B. & CORDEY, W. G. (eds) 1992. *Lithostratigraphic Nomenclature of the UK North Sea*. British Geological Survey, Nottingham.

LUNDEGARD, P. D. 1992. Sandstone porosity loss; a 'big picture' view of the importance of compaction. *Journal of Sedimentary Petrology*, **62**, 250–260.

MALLON, A. J. & SWARBRICK, R. E. 2002. A compaction trend for non-reservoir North Sea Chalk. *Marine and Petroleum Geology*, **19**, 527–539.

MALLON, A. J. & SWARBRICK, R. E. 2008. Diagenetic characteristics of low permeability, non-reservoir chalks from the Central North Sea. *Marine and Petroleum Geology*, **25**, 1097–1108.

MALLON, A. J., SWARBRICK, R. E. & KATSUBE, T. J. 2005. Permeability of fine-grained rocks: new evidence from chalks. *Geology*, **33**, 21–24.

MATTHEWS, W. J., HAMPSON, G. J., TRUDGILL, B. D. & UNDERHILL, J. R. 2007. Controls on fluviolacustrine reservoir distribution and architecture in passive salt-diapir provinces: insights from outcrop analogs. *AAPG Bulletin*, **91**, 1367–1403.

MCKIE, T. & AUDRETSCH, P. 2005. Depositional and structural controls on Triassic reservoir performance in the Heron Cluster, ETAP, Central North Sea. *In*: DORÉ, A. G. & VINING, B. A. (eds) *Petroleum Geology: North-West Europe and Global Perspectives – Proceedings of the 6th Petroleum Geology Conference*. Geological Society, London, 285–297.

MCKIE, T., JOLLEY, S. & KRISTENSEN, M. 2010. Stratigraphic and structural compartmentalization of dryland fluvial reservoirs: Triassic Heron Cluster, Central North Sea. *In*: JOLLEY, S. J., FISHER, Q. J. *ET AL.* (eds) *Reservoir Compartmentalization*. Geological Society, London, Special Publications, **347**, 165–198.

NGUYEN, B. T. T., JONES, S. J., GOULTY, N. R., MIDDLETON, A. J., GRANT, N., FERGUSON, A. & BOWEN, L. 2013. The role of fluid pressure and diagenetic cements for porosity preservation in Triassic fluvial reservoirs of the Central Graben, North Sea. *AAPG Bulletin*, **97**, 1273–1302.

OELKERS, E. H., BJORKUM, P. A. & MURPHY, W. M. 1996. A petrographic and computational investigation of quartz cementation and porosity reduction in North Sea sandstones. *American Journal of Science*, **296**, 420–452.

OSBORNE, M. J. & SWARBRICK, R. E. 1999. Diagenesis in North Sea HPHT clastic reservoir – Consequences for porosity and overpressure prediction. *Marine and Petroleum Geology*, **16**, 337–353.

PAXTON, S., SZABO, J., AJDUKIEWICZ, J. & KLIMENTIDIS, R. 2002. Construction of an intergranular volume compaction curve for evaluating and predicting compaction and porosity loss in rigid-grain sandstone reservoirs. *AAPG Bulletin*, **86**, 2047–2067.

PITTMAN, E. D. & LUMSDEN, D. N. 1968. Relationship between chlorite coatings on quartz grains and porosity, Spiro Sand, Oklahoma. *Journal of Sedimentary Petrology*, **38**, 668–670.

PITTMAN, E. D., LARESE, R. E. & HEALD, M. T. 1992. Clay coats: occurrence and relevance to preservation of porosity in sandstones. *In*: PITTMAN, E. D. (ed.) *Origin, Diagenesis, and Petrophysics of Clay Minerals in Sandstones*. SEPM Special Publications, Tulsa, USA, **47**, 241–255.

SCHNEIDER, F. & WOLF, S. 2000. Quantitative HC potential evaluation using 3D basin modelling: application to Franklin structure, Central Graben, North Sea, UK. *Marine and Petroleum Geology*, **17**, 841–856.

SMITH, R. I., HODGSON, N. & FULTON, M. 1993. Salt control on Triassic reservoir distribution, UKCS Central North Sea. *In*: PARKER, J. R. (ed.) *Petroleum Geology of Northwest Europe: Proceedings of the 4th Conference*. Geological Society, London, 547–557.

SWARBRICK, R. E. & OSBORNE, M. J. 1998. Mechanisms that generate abnormal pressures: an overview. *In*: LAW, B. E., ULMISHEK, G. F. & SLAVIN, V. I. (eds) *Abnormal Pressures in Hydrocarbon Environments*. American Association of Petroleum Geologists Memoir, Tulsa, USA, **70**, 13–34.

SWARBRICK, R. E., OSBORNE, M. *ET AL.* 2000. Integrated study of the Judy field (Block 30/7a) – an overpressured central North Sea oil/gas field. *Marine and Petroleum Geology*, **17**, 993–1010.

SWARBRICK, R. E., LAHANN, R. W., O'CONNOR, S. A. & MALLON, A. J. 2010. Role of the Chalk in development of deep overpressure in the Central North Sea. *In*: VINING, B. A. & PICKERING, S. C. (eds) *Petroleum Geology: From Mature Basins to New Frontiers – Proceedings of 7th Petroleum Geology Conference*. Geological Society, London, **1**, 493–507.

TAYLOR, T., STANCLIFFE, R., MACAULAY, C. & HATHON, L. 2004. High temperature quartz cementation and the timing of hydrocarbon accumulation in the Jurassic Norphlet Sandstone, offshore Gulf of Mexico, USA. *In*: CUBITT, J. M., ENGLAND, W. A. & LARTER, S. R. (eds) *Understanding Petroleum Reservoirs: Towards an Integrated Reservoir Engineering and Geochemical Approach*. Geological Society, London, Special Publications, **237**, 257–278.

TAYLOR, T. R., GILES, M. R. *ET AL.* 2010. Sandstone diagenesis and reservoir quality prediction: models, myths, and reality. *AAPG Bulletin*, **94**, 1093–1132.

WALDERHAUG, O. 1994. Temperatures of quartz cementation in Jurassic sandstones from the Norwegian continental shelf – evidence from fluid inclusions. *Journal of Sedimentary Research*, **64**, 311–323.

WEIBEL, R. 1998. Diagenesis in oxidising and locally reducing condition – an example from the Triassic Skagerrak Formation, Denmark. *Sedimentary Geology*, **121**, 259–276.

Wilkinson, M., Derby, D., Haszeldine, R. S. & Couples, G. D. 1997. Secondary-porosity generation during deep burial associated with overpressure leak-off: fulmar Formation, UKCS. *AAPG Bulletin*, **81**, 803–813.

Worden, R. H. & Morad, S. 2000. Quartz cementation in oilfield sandstones: a review of the key controversies. *In*: Worden, R. H. & Morad, S. (eds) *Quartz Cement in Sandstones*. International Association of Sedimentologists Special Publications, **29**, 1–20.

Worden, R. H. & Morad, S. 2003. *Clay Minerals in Sandstones: Controls on Formation, Distribution and Evolution*. Blackwell, Oxford.

Worden, R. H., French, M. W. & Mariani, E. 2012. Amorphous silica nanofilms result in growth of misoriented microcrystalline quartz cement maintaining porosity in deeply buried sandstones. *Geology*, **40**, 179–182.

Yardley, G. & Swarbrick, R. 2000. Lateral transfer: a source of additional overpressure Marine and Petroleum. *Geology*, **17**, 523–537.